Limit Cycles in a Passive Compass Gait Biped and Passivity-Mimicking Control Laws

AMBARISH GOSWAMI, BERNARD ESPIAU AND AHMED KERAMANE
INRIA Rhône-Alpes 655 avenue de l'Europe, ZIRST 38330 Montbonnot Saint Martin, France
Ambarish.Goswami@inrialpes.fr

Abstract. It is well-known that a suitably designed unpowered mechanical biped robot can "walk" down an inclined plane with a steady periodic gait. The energy required to maintain the motion comes from the conversion of the biped's gravitational potential energy as it descends. Investigation of such passive natural motions may potentially lead us to strategies useful for controlling active walking machines as well as to understand human locomotion.

In this paper we demonstrate the existence and the stability of symmetric and asymmetric passive gaits using a simple nonlinear biped model. Kinematically the robot is identical to a double pendulum (similar to the Acrobot and the Pendubot) and is able to walk with the so-called *compass gait*. Using the passive behavior as a reference we also investigate the performance of several active control schemes. Active control can enlarge the basin of attraction of passive limit cycles and can create new gaits.

Keywords: biped robot, compass gait, passive gait, limit cycle, phase plane

1. Introduction

One of the most sophisticated forms of legged motion is that of biped locomotion. From a dynamic systems point of view, human locomotion stands out among other forms of biped locomotion chiefly due to the fact that during a significant part of the human walking cycle the moving body is not in the static equilibrium. At the INRIA lab of Grenoble, France, we have started working on the development of an anthropomorphic biped walker. The envisioned prototype will have elementary adaptation capability on an unforeseen uneven terrain. The purpose of the project is not limited to the realization of a complex machine, the construction and control of which nevertheless pose formidable engineering challenge. We also intend to initiate a synergy between robotics and human gait study. Human locomotion, despite being well studied and enjoying a rich database, is not well understood and a robotic simulcrum potentially can be very useful.

In order to gain a better understanding of the inherently non-linear dynamics of a full-fledged walking machine we have found it instructive to first explore the behavior of a particularly simple walker model.

Inspired by the research of Bavarian et al. (1983) and Golliday and Hemami (1977), and the relatively more recent research on passive walking machines (McGeer, 1990) we have considered the model of a so-called "compass gait" walker. Based on the same kinematics as that of a double pendulum, the Acrobot (Berkemeier and Fearing, 1992; Spong, 1995) and the Pendubot (Block and Spong, 1995) are the nearest cousins of our compass gait model. Garcia et al. (1996) represents another recent work on a similar biped robot model.

McGeer (1990) designed, among other prototypes, a simple knee-less biped robot and studied its gravity-induced passive motion on an inclined plane. He demonstrated that the prototype can attain a stable periodic motion and analyzed this behavior with a linearized mathematical model. In order to maintain a steady locomotion the joint variables (angle, velocity) of the robot must follow a cyclic trajectory. Our objective here is to study such a passive system by means of its full non-linear equations and using tools available for non-linear systems analysis.

Underlying this somewhat local objective there are several long-term motivations all connected to the

eventual goal of obtaining a simple biologically-inspired adaptive control law for our future prototype. The first is our intuitive support of the conjecture that legged locomotion and possibly all inter-limb coordinations are identified by non-linear limit cycle oscillatory processes (Kelso et al., 1981). Next, a passive motion is enticing because it is *natural* and it does not require any external energy source. If an active control law closely mimics a passive system it is likely to enjoy certain inherent advantages of the passive system such as energy optimality, periodicity, and stability. Of particular interest in this respect is the hypothesis that a great part of the swing stage in human locomotion is passive, a hypothesis that is supported by many studies and is utilized in biped robot research (Grishin et al., 1994).

Simulation studies of our passive compass gait walker shows that such cyclic motions are represented by stable limit cycles in the phase space of the robot. We have also shown the existence of stable but asymmetric compass gait where two successive step lengths are unequal. Finally we use a passivity-mimicking control law that significantly enhances the stability robustness of the walker.

In the next section we describe the model geometry, the dynamic parameters, and the governing equations during the swing stage and the transition stage. Section 3.1 discusses with the help of a phase diagram a typical walk cycle of the passive robot on an inclined plane. The motion can continue indefinitely by maintaining a delicate balance between the robot's kinetic energy and potential energy, which we discuss in detail in Section 3.2. In Section 3.3 we show that the limit cycle associated with the periodic motion is locally orbitally stable. Section 4 introduces simple control laws for our biped and evaluates their performance. Section 4.1 presents an energy-tracking control law implemented with the hip actuator or with the support-leg ankle actuator. In Section 4.2 the control law, implemented with both the available actuators, tracks an average speed of progression of the robot, in addition to a target energy. The final section contains the conclusions and the future work.

2.   The Compass Gait Biped Model

2.1.   The Model Description and Assumptions

We consider here a very simple model of a biped robot as shown in Fig. 1. In this figure, m is the lumped mass
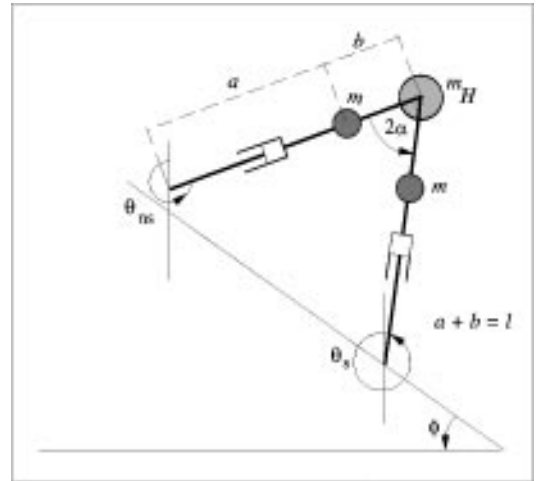

Figure 1.   Model of a compass gait biped robot on a slope.

of each leg and m_H is the hip mass. The leg-length is denoted as l which is divided into a and b, where a is the distance from the leg-tip to the position of m and b is the distance from m to the hip center. θ_s and θ_{ns} are the angles made by the biped legs with the vertical (counterclockwise positive). The total angle between the legs, which we call the "inter-leg angle" is 2α during the instant when both legs are touching the ground. The slope of the ground with the horizontal is denoted by the angle ϕ.

We have made the following assumptions in this model. All masses are considered point-masses. The legs are identical with each leg having a telescopically retractable knee joint with a massless lower leg (shank). The gait consists of a single-support or swing stage and an instantaneous transition stage. During the swing stage the robot behaves exactly like an inverted planar double pendulum with its support point being analogous to the point of suspension of the pendulum. During the transition stage the support is transferred from one leg to the other. The robot is assumed to move on a plane surface, horizontal or inclined. The impact of the swing leg with ground is assumed to be frictional inelastic. The friction is sufficient to ensure that no slip occurs between the ground and the foot.

Before proceeding further we would like to state that the compass gait robot studied here is not capable, in reality, of walking down a slope. This is because the swing leg will hit the ground during mid-swing. We attempt to avoid this conceptual problem by including the retractable massless lower leg. The telescopic retraction of the leg solves the problem of foot clearance

without affecting robot dynamics. A robot with a very similar structure has been built by Dunn and Howe (1996). Our emphasis here is more on the simplicity of the model than its physical realizability. We should also point out that the simplifying assumptions made above are routinely made in the biped robot literature (see McGeer, 1990; Hurmuzlu and Chang, 1992) and are not unique to this work.

2.2. The Governing Equations

Dynamics of the Swing Stage. As implied in the assumptions above, the biped is *always* in the swing stage except when the support is instantaneously transferred from one foot to another. The dynamic equations for the swing stage are rather well-known (see for instance, Miura and Shimoyama, 1984). Since the legs of the robot are assumed identical, the equations are similar regardless of the support leg considered. The equations have the following form:

$$M(\theta)\ddot{\theta} + N(\theta, \dot{\theta})\dot{\theta} + G(\theta) = Su \qquad (1)$$

where $M(\theta)$ is the 2×2 inertia matrix, $N(\theta, \dot{\theta})$ is a 2×2 matrix with the centrifugal coefficients, $G(\theta)$ is a 2×1 vector of gravitational torques and S is a 2×3 matrix which maps the actuator torques to the generalized coordinates. Also, $\theta = [\theta_{ns}\ \theta_s]^T$ is the vector of joint angles (see Fig. 1) and $u = [u_{ns}\ u_H\ u_s]^T$ is the vector of moments acting at the joints. The subscripts ns, H, and s denote the non-support foot, hip, and support foot, respectively. For a passive model $u = 0$.

The quantities $M(\theta)$, $N(\theta, \dot{\theta})$, $G(\theta)$, and S are of the following forms:

$$M(\theta) = \begin{bmatrix} mb^2 & -mlb\cos(\theta_s - \theta_{ns}) \\ -mlb\cos(\theta_s - \theta_{ns}) & (m_H + m)l^2 + ma^2 \end{bmatrix}$$

$$N(\theta, \dot{\theta}) = \begin{bmatrix} 0 & mlb\dot{\theta}_s \sin(\theta_s - \theta_{ns}) \\ -mlb\dot{\theta}_{ns}\sin(\theta_s - \theta_{ns}) & 0 \end{bmatrix}$$

$$G(\theta) = \begin{bmatrix} mb\sin\theta_{ns} \\ -(m_H l + ma + ml)\sin\theta_s \end{bmatrix} g$$

$$S = \begin{bmatrix} 1 & -1 & 0 \\ 0 & 1 & 1 \end{bmatrix}$$

The parameters used for our simulations are $a = b = 0.5$ m, $l = a + b$, $m_H = 2$ m $= 10$ kg.

Transition Equations. Ideally, during transition, two things happen simultaneously: the swing leg touches the ground and the support leg leaves the ground. For an inelastic no-sliding collision of the robot foot with the ground the robot's angular momentum during the collision is conserved (Hurmuzlu and Chang, 1992). This allows us to linearly relate the post-impact and the pre-impact angular velocities of the robot in the following way:

$$\dot{\theta}(T^+) = H(\theta(T))\dot{\theta}(T^-). \qquad (2)$$

$\dot{\theta}(T^-)$ and $\dot{\theta}(T^+)$ are the angular velocities just before and after the transition, which takes place at time $t = T$. Although, for simplicity, transition is assumed to be instantaneous, we should remember that in the actual physical system the hind leg must leave the ground and start swinging *only after* the front leg has hit the ground. $H(\theta(T))$ is a 2×2 matrix (henceforth referred to as H for brevity). During transition when both legs touch the ground, the inter-leg angle 2α fully defines the biped geometry. H is thus a function of α only.

The transition equations are derived from the equations $Q(\alpha)\dot{\theta}(T^+) = P(\alpha)\dot{\theta}(T^-)$ whose left hand side and the right hand sides respectively are the angular momentum of the robot after and before the impact with ground. Comparing this equation with the Eq. (2) we can write that $H = Q(\alpha)^{-1}P(\alpha)$. The matrices $P(\alpha)$ and $Q(\alpha)$ are of the forms:

$$P(\alpha) = \begin{bmatrix} (m_H l^2 + 2ml^2)\cos 2\alpha & -mab \\ -mab - 2mbl\cos 2\alpha & \\ -mab & 0 \end{bmatrix}$$

$$Q(\alpha) = \begin{bmatrix} mb^2 - mbl\cos 2\alpha & (ml^2 + ma^2 + m_H l^2) \\ & -mbl\cos 2\alpha \\ mb^2 & -mbl\cos 2\alpha \end{bmatrix}$$

We also have during the transfer:

$$\theta_{ns}(T) + \theta_s(T) = -2\phi \qquad (3)$$

and

$$2\alpha(T) = \pm(\theta_s(T) - \theta_{ns}(T)) \qquad (4)$$

where $+$ and $-$ correspond to the instants just after and just before the change of support, respectively.

3.   Characteristics of Steady Passive Compass Gaits

Simulation trials reveal that the passive compass gait robot can walk down a slope with a steady gait. A thorough analysis of this behavior is presented in Goswami et al. (1996). In Section 3.1, we describe a typical symmetric gait, using the phase diagram of the robot to identify the important time instants in a walk cycle. Next, in Section 3.2, we study in detail the interchange of the kinetic and potential energies of the robot, an interchange which characterizes its motion. Then, in Section 3.3, we study the local stability of a limit cycle.

3.1.   Description of a Typical Limit Cycle

Let us continue our discussion of the system dynamics, the existence of limit cycles, and their stability with the help of a phase portrait of the robot. The phase space of the compass gait robot is 4-dimensional. Since we cannot graphically visualize this high dimensional space we limit ourselves to a 2D projection of the robot's phase portrait. This reduced portrait involves the displacement and the velocity of only one leg. Figure 2 shows such a phase portrait of the robot after it has
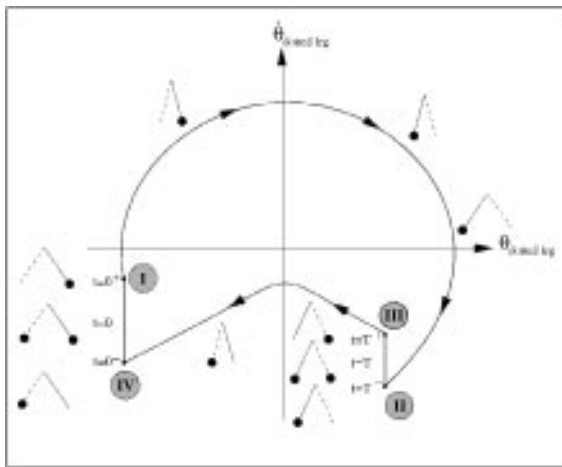

Figure 2. Phase portrait of a periodic walk. This figure corresponds to only one leg of the biped, the actual phase of the system being higher dimensional. One cycle in the figure corresponds to two steps of the robot. In the figure we have indicated some of the time stamps important in the dynamic evolution of the biped. On the outside of the cyclic portrait, the configuration of the biped has been shown with small stick diagrams. In these diagrams, one leg is dotted, the other leg is solid, and a black dot at the foot indicates the supporting leg.

walked sufficiently long such that the initial transients have settled down and the robot has settled down to a periodic gait. The leg considered alternately becomes the support leg and the swing leg. As expected, a cyclic phase trajectory is observed in the figure. Since this is a symmetric gait, the phase portrait associated with the other leg would be exactly identical.

In Fig. 2 we may start following the phase trajectory at the instant marked I corresponding to time $t = 0^+$, when the rear leg just loses contact with the ground (i.e., it becomes the swing leg). The corresponding stick diagram shows a black dot on the front foot to imply ground contact. The phase trajectory evolves in the clockwise sense in this diagram as shown by the arrowheads. While crossing the velocity axis (at a positive velocity), the biped is in the vertical configuration. Instant II corresponds to time $t = T^-$ when the swing leg is about to touch the ground. The impact between the swing foot and the ground occurs at $t = T$. We observe a velocity jump II $\rightarrow$ III due to this impact. The upper half of the cycle (I $\rightarrow$ II) depicts the swing leg suspended as a simple pendulum from a moving point (hip). At instant III ($t = T^+$), the swing leg becomes the support leg and executes the lower half of the phase plane diagram (II $\rightarrow$ III). This half of the phase portrait corresponds to the motion of the support leg "hinged" at the point of support as an inverted simple pendulum. The velocity jump of the current leg (the non-support leg of instant I) observed between IV and I is due to the impact of the other leg with the ground.

As mentioned before, Fig. 2 is a 2D projection of the complete 4D phase space. A projection of the phase space does not necessarily preserve the properties of the original phase portrait of a system. For example if we construct a 2D phase diagram of our robot before it settles down to a periodic gait we can see phase trajectories crossing each other. Crossing of two or more trajectories in the phase space of an autonomous system is impossible since that would imply that the same initial condition (the intersection point of the trajectories) can give rise to two different evolutions of the system which is un-physical. Also, the adjacency of two trajectories in a phase space projection does not necessarily imply their adjacency in the actual phase space; trajectories of equal length at two different parts of the diagrams do not necessarily imply their equality since in the higher dimensional space they may be inclined at different angles to our point of view. Some features are, however, preserved in the projection of a phase space, a very useful one being the fact that

cycles in the full phase space are also cycles (possibly self-intersecting) in its projections.

3.2. The Energy Balance in Passive Gait

As shown in Fig. 2 a passive compass biped, when started with favorable initial conditions, may walk down an inclined plane in a steady cyclic gait. We associate this to a limit cycle behavior of the non-linear system represented by Eqs. (1) and (2).

Typically, the existence of a limit cycle in a dynamical system is associated with a contraction of the phase space volume as the system evolves in time. The presence of a dissipative element in the system causes a phase space volume contraction and favors (but does not guarantee in any way) the existence of a limit cycle. Since our robot has a phase space volume conserving Hamiltonian dynamics during the swing stage we naturally search for the cause of of the existence of limit cycle. The answer lies in the impact equations (Eq. (2)). In fact, the robot mechanism behaves similar to that of a mechanical clock. In a clock the energy loss due to friction during a cycle is exactly compensated by an energy "kick" at definite intervals. For the robot the kinetic energy (KE) gain due to the conversion of gravitational potential energy (PE) in a step is absorbed in an instantaneous impact at the touchdown. Thus we see that there is, in effect, a feedback type of mechanism governing the system.

Once we have found a limit cycle we may characterize it with several parameters. For example the limit cycle shown in Fig. 2 ($\phi = 3°$) can be characterized by the step length (0.5354 m), the step period (0.734 sec) and the total mechanical energy (153.078 J). It is interesting that we have so far been unable to find two distinct stable limit cycles for the same ground slope. This indicates some underlying organizing principle which completely determines the robot's dynamic evolution once the ground slope is specified. As analytical tool for exploring such systems are not available, we can either linearize the system as in Espiau and Goswami (1993) and McGeer (1990) or do a numerical search. We do the latter here and subsequently do not claim it to be exhaustive.

Significant amount of insight may be gained from a KE vs. PE plot of the robot. Such a plot is shown in Fig. 3. In the swing stage of the robot (KE + PE) is constant and the energy trajectory (line BC) is a straight line making a 135° angle with the KE axis. The trajectory of the robot, starting from point A follows ABAC.
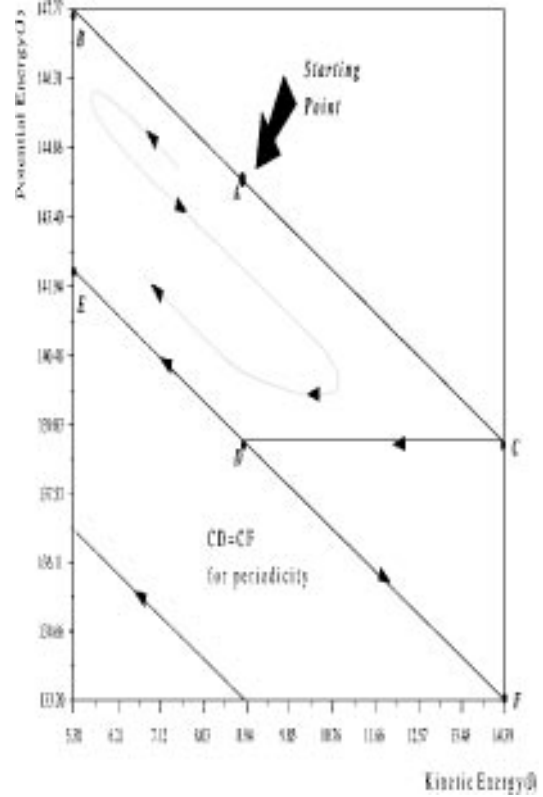

Figure 3. The KE vs. PE diagram of a compass gait. For a steady symmetric gait CD = CF.

Point C is the touchdown point where an impact occurs with the ground. The instantaneous loss of KE is shown by the line CD in the diagram. Total loss of PE in one step is given by the distance AD = CF. For a periodic gait therefore, CF = CD.

For a steady state motion on a plane of known inclination, we can calculate the amount of PE lost in each step. From Fig. 4 we see that for a symmetric step length L, the total PE lost by the robot is $(m_H + 2m)gL\sin\phi$. Since in our model $m_H = 2m$, the total PE lost can be expressed simply as:

$$PE_I - PE_{II} = PE_{III} - PE_{IV}$$
$$= \Delta PE = 4mgL\sin\phi \qquad (5)$$

We would first study the existence of periodicity of a passive biped executing a symmetric (i.e., equal left step and right step) gait. This has the advantage that the two halves of the cycle shown in Fig. 2 (half I–II–III and half III–IV–I) are identical. Thus for our subsequent studies we consider only the stages I, II, and III of
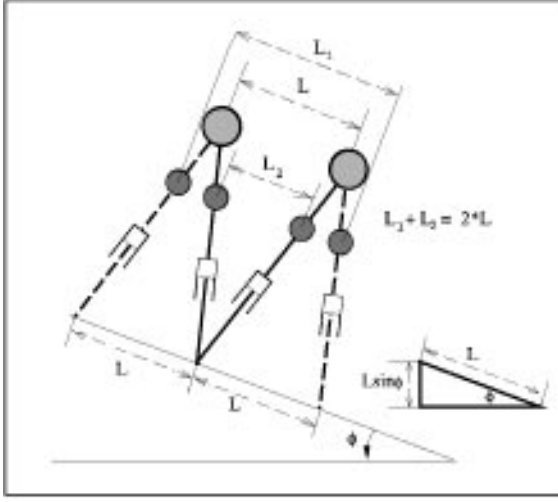
Figure 4. The figure shows one complete swing phase during which the hip mass of the robot descends by an amount $L \sin \phi$ where ϕ is the plane inclination and L is the step length. The sum of the descents of the two identical leg masses is equal to $2 \times L \sin \phi$. From this we calculate the total potential energy lost by the robot during one step.

Fig. 2. At stage III the joint positions and joint variables "initialize" themselves except for the exchange of the support leg to the stance leg and vice versa. This is expressed as

$$\theta_{III} = J\theta_{I} \tag{6}$$

$$\dot{\theta}_{III} = J\dot{\theta}_{I} \tag{7}$$

where $J = \begin{pmatrix} 0 & 1 \\ 1 & 0 \end{pmatrix}$.

One of the most fundamental parameters of a passive gait is the total mechanical energy of the robot. If the robot executes a periodic motion, the energy of the system must return to its initial value after every cycle. For a symmetric gait, the KE and the PE of the system should also initialize themselves after every half cycle. As mentioned before, the total mechanical energy of the robot is constant during the flight phase. Thus we have for stages I and II, $E_{I} = E_{II}$ where $E_{I} = PE_{I} + KE_{I}$ and $E_{II} = PE_{II} + KE_{II}$. From these we get,

$$KE_{II} - KE_{I} = PE_{I} - PE_{II} \tag{8}$$

If the system is periodic for the states I, II, and III $KE_{III} = KE_{I}$. We then obtain from Eq. (8) that

$$KE_{II} - KE_{III} = PE_{I} - PE_{II} \tag{9}$$

We remind ourselves of the *transition equations* (refer to Eq. (2))

$$\dot{\theta}_{III} = H\dot{\theta}_{II} \tag{10}$$

$$\theta_{III} = \theta_{II} \tag{11}$$

From the Eqs. (7) and (10) we can write

$$\dot{\theta}_{II} = H^{-1}J\dot{\theta}_{I} \tag{12}$$

Writing out in full the Eq. (9), we get

$$\dot{\theta}_{II}^{T}M_{II}\dot{\theta}_{II} - \dot{\theta}_{III}^{T}M_{III}\dot{\theta}_{III} = 8mgL \sin \phi \tag{13}$$

where since the robot configuration is constant during the transition (Eq. (11)), $M_{II} = M_{III}$. Now we write both $\dot{\theta}_{II}$ and $\dot{\theta}_{III}$ in terms of $\dot{\theta}_{I}$ (using Eqs. (7) and (12)) and obtain

$$(H^{-1}J\dot{\theta}_{I})^{T}M_{II}(H^{-1}J\dot{\theta}_{I}) - (J\dot{\theta}_{I})^{T}M_{II}(J\dot{\theta}_{I})$$
$$= 8mgL \sin \phi. \tag{14}$$

On simplification, this becomes,

$$\dot{\theta}_{I}^{T}J((H)^{-1}{}^{T}M_{II}H^{-1} - M_{II})J\dot{\theta}_{I} = 8mgL \sin \phi. \tag{15}$$

The last equation is in terms of the two velocity variables of the robot. If there exists a symmetric gait of step length L on a certain slope ϕ the equation gives us the relationship that must exist between the two velocity variables at the beginning of the swing stage. In other words, if we are somehow able to determine one of the velocities, the other velocity may be calculated. This equation does not help us in establishing the existence of a limit cycle in the system but rather checks the validity of a cycle once it has been identified. The information that we used in obtaining the equation is based on energy alone and does not involve the dynamics of the system in between two touchdowns. The latter would have required the integration of the non-linear equations.

3.3. Local Stability of the Limit Cycle

The concept of gait stability as applied to a walking machine is hard to define but is crucial for the performance analysis of the system. The conventional definitions of stability of a system in the sense of Lyapunov (around an equilibrium point) are not immediately suitable for

such systems. If $x(t)$ is a periodic solution of a pure autonomous robot, $x(t + \delta)$ is another solution, for every value of δ. Periodic solutions of an autonomous system cannot be asymptotically stable in the usual way. Therefore, we define below the stability of a system in terms of its *orbital stability*.

As in Hurmuzlu and Moskowitz (1986), it is natural to say that a gait is stable if, *starting from a steady closed phase trajectory*, *any finite disturbance leads to another nearby trajectory of similar shape*. Furthermore, if in spite of the disturbance, the system returns to the original cycle, the gait is called asymptotically stable.

Adapting from Hayashi (1985) we can present the notion of orbital stability in a more mathematical framework. Let us consider a continuous nonlinear system of the general form

$$\dot{x} = f(x, t). \tag{16}$$

We may eliminate time t from this equation and express the solution as a trajectory in the vector space of the states x. In this reduced space one may imagine time to be the velocity associated with the representative point along the trajectory. The phase trajectory C of Eq. (16) is said orbitally stable if, *given $\varepsilon > 0$, there is $\delta > 0$ such that*, *if R' is a representative point* (*on another trajectory C'*) *which is within a distance δ of C at time t_0, then R' remains within a distance ε of C for $t \geq 0$*. If no such δ exists, C is orbitally unstable. Analogous to the asymptotic stability of the conventional definition we may say that if the trajectory C is orbitally stable and, in addition, the distance between R' and C tends to zero as time goes to infinity, the trajectory C is asymptotically orbitally stable.

We should note that orbital stability requires that the trajectories C and C' remain near each other, whereas Lyapunov stability of the solution $x(t)$ requires that, in addition, the representative points R and R' (on C and C' respectively) should remain close to each other, if they were close to each other initially.

We have presented the nature of a stable limit cycle in the phase plane of one joint variable of the biped. As shown in the schematic representation in Fig. 5, the effect of a stable limit cycle in the phase plane will be to attract and absorb the nearby phase trajectories. A system starting from a state on the limit cycle will continue to travel on it. The shaded area in the figure indicates the region in which this attracting feature is valid. This shaded area is termed the *domain* or the
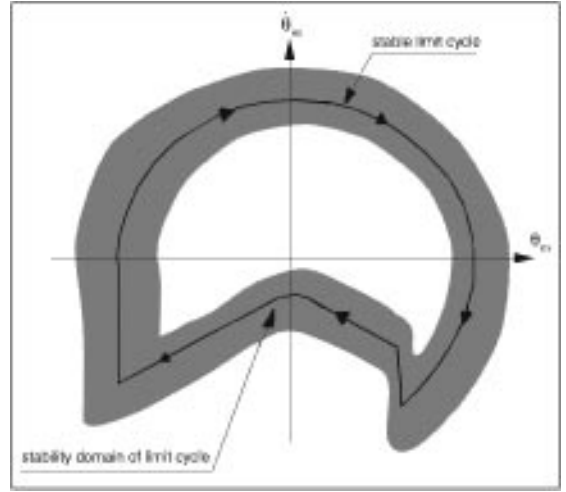

Figure 5.   Stable periodic walk. As shown in the figure, the effect of a stable limit cycle in the phase plane will be to attract and absorb the nearby phase trajectories. If the system starts from a certain state on the limit cycle, it will continue to travel on it. The shaded area shows the stable domain of the limit cycle.

basin of attraction of the limit cycle. It is interesting to note that the whole phase plane can be the basin of attraction of a limit cycle. For a certain selection of its parameters the Van der Pol oscillator exhibits this characteristic.

Finally, let us emphasize that the orbital stability of the limit cycle in Fig. 2 does not require that any of the two halves of the complete cycle (the half I $\rightarrow$ III and the half III $\rightarrow$ I) be itself a part of a closed limit cycle. In fact, the presence of a limit cycle in a differential-algebraic hybrid system such as our biped robot does not at all imply any periodic behavior in the differential part or the algebraic part of the equations. This is important for understanding the behavior of such hybrid systems. As a simple example of a hybrid system let us consider a ball bouncing on the ground. If the ball/ground impact is perfectly elastic the ball will conserve its mechanical energy and will continue to bounce indefinitely. This periodic behavior is the combined outcome of the differential motion equation as well as the impact equation of the ball. We do not see any periodic behavior if we look, for example, only at the differential part of the system which states that the downward acceleration of the ball is equal to the acceleration due to gravity. Mathematical definition and analysis of the stability of systems with impacts may be found in Gajewski and Radziszewski (1987).

One way to investigate the orbital stability of a limit cycle is by means of studying the stability of its *fixed*

point in the Poincaré map. As a natural choice of the Poincaré section of the compass biped we take the condition that the swing leg of the robot touches the ground. For two successive touchdowns of the same leg the states of the robot can be related as

$$x_k = F(x_{k+1}) \qquad (17)$$

where $x = [\theta_{ns} \; \theta_s \; \dot{\theta}_{ns} \; \dot{\theta}_s]^T$ is the 4-component state vector of the robot.

For a cyclic phase trajectory the first return map is the fixed point of the mapping. On a cyclic trajectory, therefore, $xk = x_{k+1}$ and we can write, $x^* = F(x^*)$. For a small perturbation Δx^* around the limit cycle the nonlinear mapping function F can be expressed in terms of Taylor series expansion as

$$F(x^* + \Delta x^*) \approx F(x^*) + (\nabla F)\Delta x^* \qquad (18)$$

where ∇F is the gradient of F with respect to the states. Since x^* is a cyclic solution, we can rewrite Eq. (18) as

$$F(x^* + \Delta x^*) \approx x^* + (\nabla F)\Delta x^* \qquad (19)$$

The mapping F is stable if the first return map of a perturbed state is closer to the fixed point. This property can be viewed as the contraction of the phase space around the limit cycle. Mathematically this means that the modulii of the eigenvalues of ∇F at the fixed point x^* are strictly less than one. From Eq. (19) we write $(\nabla F)\Delta x^* \approx F(x^* + \Delta x^*) - x^*$ where $F(x^* + \Delta x^*)$ is the first return map of the perturbed state $x^* + \Delta x^*$. As it is not practical to analytically calculate the matrix (∇F) we will do so numerically. One straightforward method is to perturb one state at a time by a small amount and observe its first return map. Repeating this procedure at least four times (once for each of the four states) we obtain an equation of the form

$$(\nabla F)\tau = \Psi \qquad (20)$$

where the 4 × 4 diagonal matrix τ contains as its diagonal entries the perturbations of the state variables (Δx_i^*). The ith column of the 4 × 4 matrix Ψ gives in terms of the four states how far away from the periodic solution the first return map shows up due to a perturbation of the ith state variable. Assuming that τ is non-singular, computation of ∇F is straightforward: $\nabla F = \Psi \tau^{-1}$.

As an example, we have derived the value of ∇F for the compass with $2m = m_H = 10$ kg and $a = b = 0.5$

meter walking with a steady passive gait on a 3° downward incline. We have obtained:

$$\nabla F = \begin{bmatrix} -0.439 & -0.500 & -0.003 & -0.169 \\ 0.439 & 0.500 & 0.003 & 0.169 \\ 0.147 & -2.933 & 0.082 & -1.065 \\ -0.877 & -1.846 & 0.011 & -0.633 \end{bmatrix}$$
$$(21)$$

with eigenvalues

$$\begin{array}{c} -0.252 + 0.215i \\ -0.252 - 0.215i \\ 2.554 \times 10^{-9} \\ 0.014 \end{array} \qquad (22)$$

Their absolute values are $0.332, 0.332, 2.554 \times 10^{-9}$, and 0.014. Thus the cycle is stable. As expected (Ott, 1993) we have a zero eigenvalue. The eigenvector associated with this eigenvalue is directed locally along the limit cycle. Thus a finite perturbation along this eigenvector reduces to a zero perturbation in the first return map since the perturbed point continues to stay on the limit cycle.

We note here that the mere fact that we have found a limit cycle by means of numerical simulation practically guarantees that the cycle is stable. Unless we *accidentally* hit the exact states on an unstable limit cycle they are never visible in numerical trials.

One curious thing happens for slightly higher slopes. As we show in Fig. 6 there is a bifurcation of the solution and the robot exhibits a limit cycle which repeats itself every *two* cycles. Physically this means two successive robot steps are not identical. A local stability analysis of the fixed point, which is, in this case,
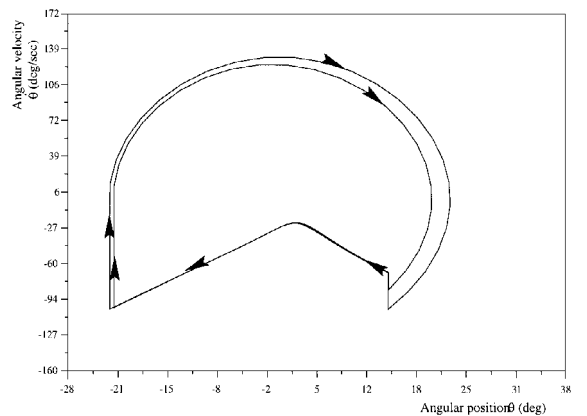

Figure 6.   Phase portrait of a stable passive asymmetric walk.

the position on the Poincaré section where the phase trajectory intersects every other time, shows that this 2-periodic gait is stable. Detailed investigation on these "unsymmetric" gaits have been performed (Goswami et al., 1996).

4. Two Different Control Laws

In this section we present two different control laws for the compass gait biped: one law tracks a given mechanical energy of the robot and the other tracks, in addition, a specified average progression speed.

4.1. Control Law Tracking Passive Energy Level

Here we introduce a simple control law which was inspired by the passive energy characteristics of the compass model. Please recall that as the robot walks down on a slope its support point also shifts downward at every touchdown. As it loses gravitational potential energy in this way its kinetic energy increases accordingly. In a steady walk this is exactly the amount of kinetic energy that is to be absorbed at the end of each step by the impact. If, at every touchdown we reset our potential energy reference line to the point of touchdown, the total energy of the robot appears constant regardless of its downward descent. We formulate a control strategy for the robot based on this principle. The control law, aware of this characteristic energy of the passive limit cycle, called the *reference energy* in this section, of the robot on a given slope, tries to drive the robot toward it.

The approach assumes that for the given slope a passive limit cycle exists and that we have already identified it. Although this may appear extremely constraining at first, we will subsequently see that one of the advantages of active control is that it is able to generate gaits which do not exist for the unpowered robot. We must point out at the same time that the control laws presented in this section function well only in the neighborhood of the passive gait and their performance deteriorate as we go further away (in terms of energy, speed, etc.) from the natural motion. This, as well as our inability to find two different passive gaits on the same slope, indicates that there is a strong inherent rationale for the robot to choose the particular passive gait it chooses.

The total mechanical energy E of the robot can be expressed as $E = 0.5\dot{\boldsymbol{\theta}}^T \boldsymbol{M} \dot{\boldsymbol{\theta}} + \text{PE}$. The power input to the system is the time rate of change of total energy, $\dot{E} = \dot{\boldsymbol{\theta}}^T \boldsymbol{S} \boldsymbol{u}$ where $\boldsymbol{u}$ and $\boldsymbol{S}$ have their usual meanings (see Eq. (1)). For a passive cycle, $\boldsymbol{u} = \boldsymbol{0}$ and the reference energy $E^* = E(\dot{\boldsymbol{\theta}}^*, \boldsymbol{\theta}^*)$. Suppose now that we use a simple damper control law of the form $\boldsymbol{S}\boldsymbol{u} = -\beta\dot{\boldsymbol{\theta}}$. The power input to the system is therefore $\dot{E} = -\dot{\boldsymbol{\theta}}^T \beta \dot{\boldsymbol{\theta}}$. For a positive definite β, the quantity $-\dot{\boldsymbol{\theta}}^T \beta \dot{\boldsymbol{\theta}} < 0$ which means that the robot's energy decreases monotonically. In order to simplify our choice, let us specify that our control law should attempt to bring the current energy level of the robot to the reference energy level at an *exponential* rate.

At any instant at most two actuators are available to actuate the robot—the hip actuator and the actuator in the supporting leg at the point of support ("support ankle torque"). There are thus three ways of implementing the control law, by means of the two actuators acting independently or them acting together. We will study the energy tracking control law with an independent hip actuator and an independent support leg actuator and later study an improved control law employed with both actuators. The next subsection studies the performance of the control law with only a hip actuator.

Control with Hip Torque. We propose a control law of the following form:

$$\dot{E} = -\lambda(E - E^*) = \dot{\boldsymbol{\theta}}^T \boldsymbol{S} \boldsymbol{u} = [\,\dot{\theta}_{ns} \quad \dot{\theta}_s\,] \begin{bmatrix} -u_H \\ u_H \end{bmatrix} \tag{23}$$

from which we can calculate

$$u_H = -\frac{\lambda(E - E^*)}{\dot{\theta}_s - \dot{\theta}_{ns}} \tag{24}$$

Larger the value of λ faster is the rate of convergence to the reference energy level. The control law has a singularity at $\dot{\theta}_s - \dot{\theta}_{ns} = 0$ and this condition must be taken into account, for example, by setting the control to zero whenever $\|\dot{\theta}_s - \dot{\theta}_{ns}\| < \varepsilon$.

In Fig. 7 we show an active phase cycle superimposed on the passive limit cycle obtained on a $3°$ slope. The advantage of the active control becomes clear when we note that the starting position shown in the figure lies outside the basin of attraction of the passive limit cycle. In other words the passive robot would have fallen down soon had it started from this initial condition. The
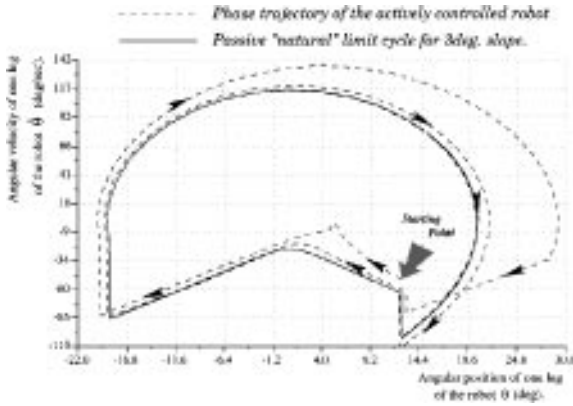
Figure 7. Active stabilization of a limit cycle. Here we show the performance of the energy tracking control law for a robot walking down on a 3° slope. The system driven only by a hip torque seeks and returns to the passive cycle of the robot. The initial conditions from which the system is brought to the limit cycle lie outside the basin of attraction of the passive limit cycle.

control law has thus enlarged the basin of attraction of the passive limit cycle.

Next, we deliberately attempt to create unnatural limit cycles on a 3° slope by means of specifying a target mechanical energy E^{tar} which is different from the reference energy corresponding to that slope.

The most remarkable feature of this control law is the fact that although it produces new gaits it does not completely succeed in tracking the specified target energy. In all cases, the robot settles down to a cycle with an energy which is close but different from the reference energy. In Table 1 we show the important parameters of the resulting steady gait (inter-leg angle, average speed of progression, step period, and the final settling energy) for different target energies. The first row of

Table 1. Active biped gait parameters for different target energies, E^{tar}. The parameters considered are the half inter-leg angle α, the average speed of progression v, the step period T, and the energy level at which the robot converged at the end. For this table $\lambda = 0.1$.

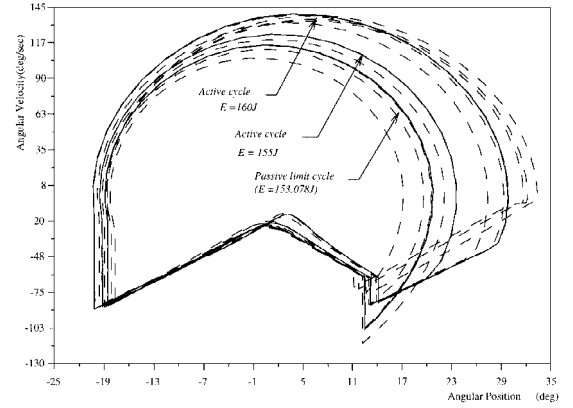| E^{tar} (J)	α (°)	v (m/s)	T (s)	E_{final} (J)
153.08	15.53	0.729	0.73	153.08
155	16.19	0.713	0.78	153.15
157	16.53	0.693	0.82	153.15
158	16.72	0.681	0.84	153.14
160	17.16	0.646	0.91	153.09
162	17.82	0.576	1.06	152.96

Figure 8. Energy tracking control using hip actuator.

the table corresponds to the convergence of the actively controlled robot into the passive limit cycle. The table shows that regardless of the value of the target energy, the final settling energy value is close to that of the reference "passive" energy level. The resulting cycles are, however, quite different as can be seen from the change in the other pertinent parameters of the cycles. For the results in this table the value of λ was held fixed at 0.1.

Figure 8 shows the phase portrait of one leg of the robot for three different target energies (the 1st, the 2nd, and the 5th rows of Table 1). Note that the major effect of the control seems to be limited during the second-half of the swing stage. This is because of the fact that the hip torque influences the swing leg of the robot more readily than it does to the stance leg. If we increase the gain λ for the same target energy, the robot slows down and executes larger steps. This is because a larger λ causes a higher tracking error which directly sets into motion the swing leg. However this is not associated with a corresponding increase in the support leg motion and thus the step length tends to increase.

In conclusion we mention that no cycle with an energy level E^{tar} less than that corresponding to the passive cycle could be generated.

Control with Ankle Torque. In this section we implement the same control law employing only the support ankle torque. Following the same procedure as in Eq. (23) we can derive,

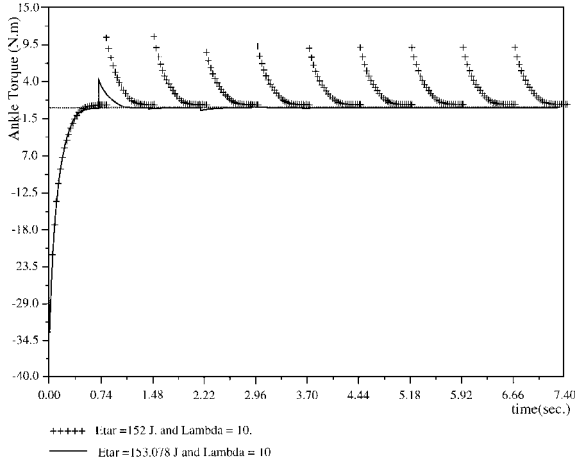$$u_s = -\frac{\lambda}{\dot{\theta}_s}(E - E^*). \qquad (25)$$

Figure 9. Energy tracking control using support ankle actuation. 10 steps of the robot is recorded here. The support ankle alternates between the left ankle and the right ankle.

Figure 9 shows the evolution of ankle torque, the control input. The repeated peaks in the control torque correspond to the time instants of foot touchdown. The zero of the time axis in the figure corresponds to the beginning of a swing stage. We see that the control is active from the beginning and near the end of this stage the control becomes zero as the robot's energy reaches the reference energy. Foot touchdown causes a sudden change in the angular velocities and thus the system energy, thereby necessitating an injection of control input. Figure 10 shows a phase plane cycle of the robot using this control. In comparing with Fig. 8 we see that the form of the phase portraits of the robot
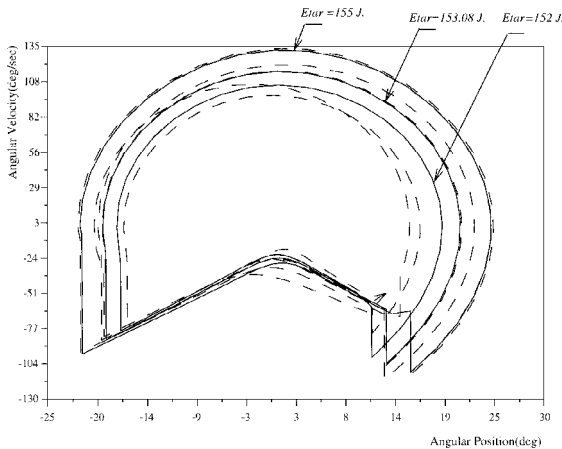

Figure 10. Phase plane representation of the energy tracking control using support ankle actuation.

gait with ankle torque control resembles much more to those of the passive robot.

We should remember that in reality arbitrarily large ankle torques cannot be applied as this may cause the robot foot to roll on the ground or perhaps leave the ground.

The main difference between the ankle torque control and the hip torque control is that with the former we can effectively converge to any target energy (within a limit) which is not possible with the latter. Intuitively this makes sense since the ankle torque is capable of more directly affecting the overall dynamics of the robot. Whether controlled at the hip or at the ankle, the control law enlarges the basin of attraction of the limit cycle.

4.2. Control of Average Progression Speed

Step-to-Step Energy Tracking. Although the single-actuator control laws studied in the previous section are capable of creating steady gaits, their performance is limited by the fact that the generated gaits are still close to the passive gait. In other words, if we specify a target energy which is very different from the reference energy, the control law cannot generate a corresponding active cycle. In order to improve the robot performance we propose a control law which attempts to maintain, in addition, a specified average speed of progression.

The average speed per step is given by $v = \frac{2l\sin(\alpha)}{T}$. The target energy at the kth step, E_k^{tar}, is equal to that at the $(k-1)$th step with an added term which is proportional to the error in speed. E_k^{tar} is thus expressed as

$$E_k^{\text{tar}} = E_{k-1}^{\text{tar}} + \eta(v^{\text{tar}} - v_{k-1}), \qquad (26)$$

where η is a weighting factor between energy and speed. The active cycle, implemented with both the actuators, is thus parameterized by the target energy and the average speed. A simplification is obtained by imposing that the hip torque be proportional to the ankle torque with a proportionality constant of μ. Thus $\boldsymbol{u} = [1\ \mu]^T u_H$. Following the same approach as in Eq. (23) we can write,

$$u_H(\dot{\theta}_s(1+\mu) - \dot{\theta}_n) = -\lambda\left(E - E_k^{\text{tar}}\right)$$

As E_k^{tar} is given by Eq. (26), the control law is $u_s = \mu u_H$ and

Table 2. Effect of λ on the control performance. The table corresponds to simulations on a 3° slope with parameters: $\mu = 5, \eta = 2$, $E_0^{\text{tar}} = 153$ J, and $v^{\text{tar}} = 0.5$ m/s.

λ	α (°)	v (m/s)	T (s)	E_{final} (J)
5	9.94	0.5	0.69	148.98
10	10.56	0.5	0.73	149.45
20	10.83	0.5	0.75	149.72
50	10.94	0.5	0.76	149.86
100	10.96	0.5	0.76	149.90

$$u_H = \begin{cases} -\frac{\lambda}{\dot{\theta}_s(1+\mu)-\dot{\theta}_n}(E - E^{\text{tar}}) & \text{if } \|\dot{\theta}_s(1+\mu) - \dot{\theta}_n\| > \varepsilon \\ 0 & \text{otherwise} \end{cases}$$

(27)

Control Performance under Parameter Variations.
Control of the average speed with two actuators ensures the convergence to an active cycle for a reasonably specified speed. We study the control law in detail by changing one parameter at a time while holding the others fixed. The parameters concerned are λ, μ, η, and E_0^{tar}.

Effect of λ. The following simulations are conducted for a 3° slope with $\mu = 5, \eta = 2, E_0^{\text{tar}} = 153$ J, and $v^{\text{tar}} = 0.5$ m/s. The natural velocity for the passive cycle is 0.73 m/s. The results are summarized in Table 2. The table shows the values of the inter-leg angle, the average speed, the step period, and the mechanical energy of the robot after 100 steps when it is assumed that the robot has settled to a steady gait.

As shown in the table the desired average speed is reached for a large range of values of λ. As the target speed is less than that corresponding to the passive limit cycle, the robot tries to lengthen its step length and the step period to maintain a constant average speed.

Effect of μ. The most curious effect of μ is that for higher values it causes a bifurcation leading to asymmetric or 2-periodic gaits. In such a gait the average speed oscillates around the target speed, the amplitude of this oscillation increases with μ. For the results in the following table $\lambda = 5, \eta = 5$, and $E^{\text{tar}} = 153$.

Effect of η. If $\eta = 0$, the target energy is not updated at every step so for a target energy equal to the reference energy the robot converges to the passive limit cycle. Otherwise η slightly affects the speed of convergence to the cycle.

Table 3. Effect of μ on the control performance. The table corresponds to simulations on a 3° slope with parameters: $\lambda = 5, \eta = 5$, and $E^{\text{tar}} = 153$ J.

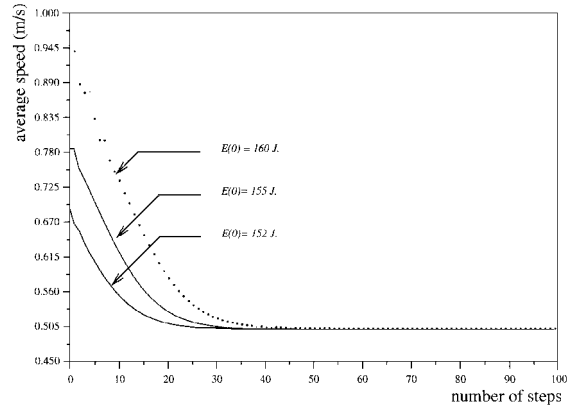| μ	α (°)	v (m/s)	T (s)
5	9.942	0.5	0.69
15	10.831	0.5	0.75
20	10.901	0.5	0.76
30	10.21 and 11.51	0.499 and 0.501	0.71 and 0.79
60	9.86 and 11.69	0.496 and 0.504	0.68 and 0.82

Figure 11. Convergence towards the target average speed of 0.5 m/s for different starting target energies.

Effect of Starting Target Energy E_0^{tar}. As shown in Fig. 11 the major effect of E_0^{tar} is in the rate of convergence to the target speed. Note that the target energy is modified at every step and we cannot predict a-priori to what final energy the robot will converge.

Walking up a Slope. The speed control law was also tested for upward slope walking. We have supposed as before, that collision with the ground is avoided by means of the retraction of the massless shank of the swing leg. The following table summarizes some simulations for different slopes with $\lambda = 6.95, \mu = 3.2, \eta = 2$, and $E_0^{\text{tar}} = 153$ J.

In general if the inclination of the upward slope is increased the robot tends to lengthen the step length in order to maintain the specified speed. A typical walk of the robot up a slope of 12° is shown in Fig. 12. We can easily extend the same control law to control the robot on a terrain with a series of plane surfaces with changing slopes. In case of 12° slope increasing μ to 5.2 makes the robot avoid the bifurcation phenomenon which was observed for the 10° slope.

Table 4. Speed control for upward walk. Effect of μ on the control performance. The table corresponds to simulations with parameters: $\lambda = 6.95$, $\mu = 3.2$, $\eta = 2$, and $E_0^{\text{tar}} = 153$ J.

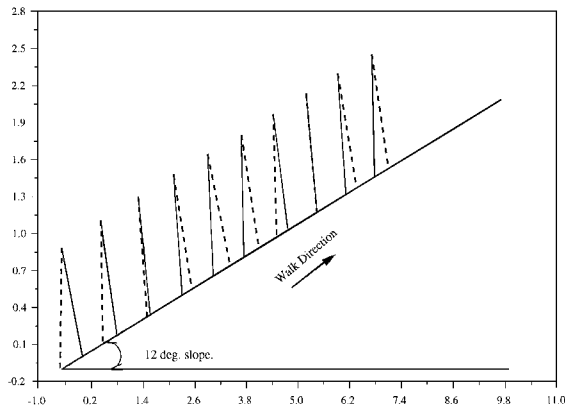| ϕ (°)	α (°)	v (m/s)	T (s)
5	10.51	0.5	0.73
7	10.65	0.5	0.74
10	13.99 and 8.21	0.440 and 0.559	0.65 and 0.86
12 ($\mu = 5.2$)	9.44	0.5	0.66

Figure 12. Upward walk of the biped on a 12° slope—control of the average progression speed with two actuators.

5. Conclusions and Future Work

We have studied the stability and the periodicity properties of the passive motion of a simple biped machine, the compass gait walker. We have shown that such a biped can walk down on an inclined plane in a steady periodic fashion. There is a strong indication that all the motion descriptors of such a gait are determined by only one parameter, the slope of the inclined plane. A rigorous proof of this fact has, so far, been elusive. The motion equations exhibit a bifurcation phenomenon at a certain slope angle when a symmetric periodic motion changes to another stable periodic motion with unequal step lengths. Further investigation is required on this topic.

Although not useful as a viable walk, the *unstable* limit cycles of the robot may tell us more about its global properties. In order to identify the unstable limit cycles we would need to integrate the system back in time.

We should remember that robot's behavior is heavily influenced by our impact model which is not, by any means, the only available impact model. In order

to control a real robot we have two main options—to model the foot/ground impact in such a manner that reasonable perturbations of the model parameters do not dramatically change the gait. If it does, the model cannot be deemed reliable. A second option is to select a foot material such that there is no significant impact during the robot's touchdown.

For control purposes, it will be useful to identify the boundary of the basin of attraction and to determine the favorable initial conditions. In order for a control law to be robust and reliable the limit cycle associated with it should have a reasonably wide basin of attraction.

We have introduced a simple control law in the spirit of the passive characteristics of the robot motion and demonstrated that the basin of attraction of the limit cycle can be significantly enlarged by the introduction of even one control input.

The proposed control generated "unnatural" but stable gait cycles. We were also able to track different target speeds, slower and faster than that corresponding to the passive gait. With speed-tracking control, robot also walked up a slope.

The present study can be considered as a precursor of our exploration of simple biologically inspired control laws for a multi dof anthropomorphic robot prototype.

References

Bavarian, B., Wyman, B.F., and Hemami, H. 1983. Control of the constrained planar simple inverted pendulum. In *International Journal of Control*, 37(4):741–753.

Berkemeier, M.D. and Fearing, R.S. 1992. Control of a two-link robot to achieve sliding and hopping gaits. In *Proc. of IEEE Conf. on Robotics and Automation, Nice*, Vol. 1, pp. 286–291.

Block, D.J. and Spong, M.W. 1995. Mechanical design & control of the pendubot. In *Proc. of SAE Earthmoving Industry Conference*, Peoria, IL.

Dunn, E. and Howe, R.D. 1996. Foot placement and velocity control in smooth bipedal walking. In *IEEE International Conference on Robotics and Automation*, Minneapolis, MN, U.S.A.

Espiau, B. and Goswami, A. 1993. Compass gait revisited. In *Proc. of the Symposium of Robot Control (SyRoCo)*, Capri, Italy.

Gajewski, K. and Radziszewski, B. 1987. On the stability of impact system. *Bulletin of the Polish Academy of Sciences*, 35(3/4):183–189.

Garcia, M., Chatterjee, A., Coleman, M., and Ruina, A. 1997. The simplest walking model: Stability, complexity, and scaling. *ASME Journal of Biomechanical Engineering* (accepted).

Golliday, C.L. and Hemami, H. 1977. An approach to analyzing biped locomotion dynamics and designing robot locomotion controls. *IEEE Trans. on Aut. Cont. AC*, 22(6):964–972.

Goswami, A., Thuilot, B., and Espiau, B. 1996. Compass-like biped robot Part I: Stability and bifurcation of passive gaits. Technical report, INRIA, No. 2996.

Grishin, A.A., Formal'sky, A.M., Lensky, A.V., and Zhitomirsky, S.V. 1994. Dynamic walking of a vehicle with two telescopic legs controlled by two drives. *International Journal of Robotics Research*, 13(2):137–147.

Hayashi, C. 1985. *Nonlinear Oscillations in Physical Systems*. Princeton University Press: Princeton, NJ.

Hurmuzlu, Y. and Moskowitz, G.D. 1986. The role of impact in the stability of bipedal locomotion. *Dynamics and Stability of Systems*, 1(3):217–234.

Hurmuzlu, Y. and Chang, T.-H. 1992. Rigid body collisions of a special class of planar kinematic chains. *IEEE Transactions on Systems, Man, and Cybernetics*, 22(5):964–971.

Kelso, J.A.S., Holt, K.G., Rubin, P., and Kugler, P.N. 1981. Patterns of human interlimb coordination emerge from the properties of non-linear, limit cycle oscillatory processes: Theory and data. *Journal of Motor Behavior*, 13(4):226–261.

McGeer, T. 1990. Passive dynamic walking. *Int. J. of Rob. Res.*, 9(2):62–82.

Miura, H. and Shimoyama, I. 1984. Dynamic walk of a biped. *Int. J. of Rob. Res.*, 3(2):60–74.

Ott, E. 1993. *Chaos in Dynamical Systems*. Cambridge University Press: UK.

Spong, M. 1995. The swing up control problem for the acrobot. *IEEE Control Systems Magazine*.

Bernard Espiau graduated from the Ecole Nationale de Mécanique de Nantes, France in 1972. He received the "Docteur-Ingénieur" in automatic control and the "Docteur d'Etat" in applied mathematics grades in 1975 and 1981, respectively.

As a Research Director, he was the head of a robotics project in the Rennes Laboratory of INRIA until 1988. From 1988 to 1992 he was Director of the Institut Supérieur d'Informatique et Automatique, an educational institute in Sophia Antipolis, and Associate Professor at the Ecole des Mines de Paris. He is presently in charge of scientific aspects at the INRIA center of Grenoble and head of the INRIA project BIP. His current research interests are legged robot control, biomechanics and verification and programming issues. B. Espiau has published more than 60 papers: Conferences, Journals, Book chapters. With C. Samson and M. Le Borgne, he is also co-author of the book *Robot Control: The Task-Function Approach* (Clarendon Press, Oxford, England, 1991). He is a member of several Conference Program Committees, e.g., IEEE Conf. on Robotics and Automation, and is the Chairman of the 1997 IFAC Symposium on Robot Control. He serves as an Associate Editor to the IEEE Transactions on Control Systems Technology.

Ambarish Goswami received the Bachelor's degree from Jadavpur University, Calcutta, India, the Master's degree from Drexel University, and the Ph.D. degree from Northwestern University all in Mechanical Engineering. During his doctoral study under the direction of Michael Peshkin he worked on automated assembly, programmable passive mechanical devices, robot calibration, and computer assisted surgery. Following his graduation he spent a year as Post-Doctoral Research Fellow in the INRIA Rhone-Alpes Laboratory in Grenoble, France, where he is currently employed as Chargé de Recherche, a member of the permanent scientific staff. His current area of research includes legged locomotion in machine and human, biped robots, optimal control, and impacting systems.

Ahmed Keramane was born in Algeria in 1966. He received the B.Sc. degree in Electrical Engineering from the Department of Control at The National Engineering and Technical School of Algeria (ENITA) in 1989 and the MSEE from the Control Systems Laboratory of Grenoble (LAG) in 1990. Presently, he is a Ph.D. student at the National Research Institute in Computer Science and Control (INRIA). His research interests include simulation of discrete-continuous systems, passive locomotion, control of underactuated robots, biped robotics.